Computers & Structures Vol. 33, No. 4, pp. 1095–1106, 1989
Printed in Great Britain.

0045-7949/89 $3.00 + 0.00

DISPLACEMENT AND STRESS PREDICTIONS FROM FIELD- AND LINE-CONSISTENT VERSIONS OF THE EIGHT-NODE MINDLIN PLATE ELEMENT

B. P. NAGANARAYANA and G. PRATHAP
Structural Sciences Division, National Aeronautical Laboratories, Bangalore 560017, India

(*Received* 3 *November* 1988)

Abstract—The eight-node isoparametric Mindlin plate bending element based on the serendipity shape functions has a long history of investigation behind it, and has seen various devices to improve it—mixed methods, enforcing of constraints, tensorial transformations, etc. Only very recently have successful versions free of locking in general quadrilateral form and without kinematic modes emerged. In this paper, we shall examine two of the most successful displacement method procedures (a field-consistency approach and a line-consistency approach) and proceeding from these, design three very accurate versions—one based on a variationally correct field-consistency paradigm alone, and two versions derived from the need to ensure consistency of tangential shear strains along principal reference lines so that the usual patch tests are exactly passed. The latter two have shear strain definitions that leave the element free of all problems (locking and kinematic modes) for all boundary suppressions and element distortions whereas the former has two kinematic modes. These line-consistent elements, however, introduce spurious quadratic shear stress oscillations as they have not been derived in a variationally correct sense. The recovery of accurate transverse shear stress resultants must therefore be performed very carefully, and a filtering technique is implemented for this.

INTRODUCTION

Survey

Simple Mindlin plate bending elements [1] are very popular as they can account for transverse shear strain deformation and yet need only C° continuous functions for the engineering degrees of freedom: the displacements and section rotations.

The eight-noded element based on the serendipity interpolation functions has been a very tricky one to design. The conventional approach of exact integration of all strain energies (as derived from the Ahmad shell element [2]) resulted in an element that locked for most practical boundary suppressions even in its rectangular form. Many *ad hoc* techniques e.g. the reduced and selective integration techniques [3–5], hybrid and mixed methods [6], etc. failed or succeeded only partially. Very recently, the use of special interpolation strategies for shear strains [7–9] led to elements that did not lock even under distortion and without inducing zero-energy or kinematic modes.

References [7] and [8] use a covariant base approach. These formulations ensure that the constraints emerge from interpolations in the natural co-ordinates for a covariant natural co-ordinate based shear strain tensor system. These are then transformed to shear strains in the Cartesian co-ordinate system using tensorial transformations or even with Jacobian transformations such that 'consistency' is preserved. However, the assumed strain interpolations are based on sampling at five optimal points (Hinton and Huang [8]) and although the element is free of locking in its distorted form and passes the patch tests exactly, it has low accuracy in both displacement prediction and stress recovery, and slow convergence. We shall show in this paper that the poor accuracy in displacement prediction is due to the use of a five-point sampling strategy in setting up the assumed shear strain interpolations and that the use of least squares accurate satisfaction of shear strain consistency along the principal reference lines can produce a better element. However, these assumed strain definitions are still not field-consistent over the element domain in a variationally correct sense and this leads to spurious transverse shear stress oscillations and, hence, apparently very poor transverse shear stress prediction capability.

Donea and Lamain [9] set up the consistent interpolation functions for the transverse shear strains in the Cartesian system itself by very cleverly identifying the polynomial forms in the natural co-ordinates required to ensure that these shear strains in the Cartesian co-ordinate system satisfy the consistency requirements on the principal reference lines. The coefficients multiplying the sets of polynomial functions are determined to approximate, in a mean value accurate sense, the transverse shear strain fields derived from the displacement fields along such lines. This appears to be the most complete description of shear flexible quadrilateral plate elements that can be found which is line-consistent and free of all zero-energy mechanisms. We shall attempt to show that it should be possible to produce an element in the covariant base approach that will have the efficiency of Donea and Lamain's element by using the line-consistency approach with a careful identification of

the consistency needs when the serendipity functions are used. These elements have a displacement prediction capability that is markedly superior to the Hinton and Huang element. Again, these line-consistent elements are not based on assumed strain distributions which are variationally equivalent over the entire element domain to the Hellinger–Reissner (HR) or Hu–Washizu (HW) descriptions and this leads to significant quadratic shear stress oscillations, and seemingly poor transverse shear stress predictions. This demands a suitable filtering procedure to pick up the correct shear stress resultants.

Field-consistency and the variationally correct way to derive assumed strain fields over an element domain

The 'field-consistency' requirements of constrained media problems [10, 11] were the basis for the use of various substitute shear strain interpolation strategies for the QUAD8 element in a recent study [12]. The 'consistent' substitute shear strain fields (or assumed shear strain fields) were obtained from a least squares field-redistribution technique from the 'inconsistent' shear strain-fields from the kinematically admissible displacement fields. It was recently established that a variational basis exists for this procedure [13, 14].

Briefly, the argument for this procedure runs as follows. The field-consistency paradigm [10, 11] recommends the form of the assumed strain functions in terms of the independent space variables such as x, y or ξ and η as the case may be, so that they are 'field-consistent', i.e. no spurious constraints develop in the constraining limits. References [13] and [14] show how an orthogonality condition can be derived from the Hellinger–Reissner or Hu–Washizu theorem which determines the constants for the 'consistent' assumed strain field from the constants of the strain fields derived directly from the displacement fields. For variational correctness or equivalence, the orthogonality condition demands that the assumed strain field must be orthogonal to the difference between the assumed strain field and the strain field resulting from the chosen displacement field. The redistribution procedure used to determine an admissible assumed shear strain field in the case of isotropic Mindlin plate theory is orthogonally correct if a least squares smoothing over the element domain is performed to arrive at the constants of the assumed strain function. However, if the assumed strain functions have been generated without reference to this requirement, as is the case with the various line-consistent formulations, the variational correctness is lost and spurious energy or loading terms are introduced [15].

However, it was seen that this simple application of the least squares accurate smoothing technique to derive what seemed to be orthogonally correct field-consistent forms (QUAD8-1 and QUAD8-2 of Ref. [12]) still failed to remove locking, and when it succeeded (QUAD8-3 of Ref. [12]), was at a level that also introduced two zero-energy modes. The line-consistent elements, on the other hand, were free of such zero-energy mechanisms.

Another aspect that needs consideration is the performance of the element when it is distorted into arbitrary quadrilateral form. Formulations using the covariant base [7, 8] have succeeded in retaining consistency under such distortions. The line-consistent elements [8, 9] are particularly successful in this. A parallel investigation of the four-noded plate element pointed to the additional need for consistency of tangential shear strains along edge lines [16] and showed that it was possible to synthesize the optimal shear strain interpolations needed to produce a four-node Mindlin plate bending quadrilateral that was free of locking even in its most distorted form, i.e. when it was collapsed into a triangle.

We find that the synthesis of field- and line-consistency requirements for Lagrangian elements (i.e. four-node and nine-node elements, etc.) does not lead to any conflicting requirements and gives elements free of any difficulties because they are variationally equivalent to the Hellinger–Reissner or Hu–Washizu theorems [13]. However, when we try to extend these arguments to discover the field- and line-consistent forms of the interpolation functions for the shear strains in the covariant base that will ensure that the eight-noded element will not lock, we find that we must compromise on the need to obtain the variational equivalence to the HR or HW principle and the element that results, although having very accurate displacement predictions also leads to noticeable spurious quadratic shear stress oscillations. It is therefore necessary to examine carefully how the shear stress resultants can be accurately derived from the displacement fields.

DESCRIPTION OF ELEMENT

Let us first consider the setting up of the description of Mindlin plate bending theory using the serendipity eight-noded C° continuous shear flexible element. It needs three nodal degrees of freedom: w, θ_x and θ_y at eight nodes [see Fig. 1(a)]. The curvatures and shear strains are:

$$\chi_x = \theta_{x,x}$$

$$\chi_y = \theta_{y,y}$$

$$\chi_{xy} = \theta_{x,y} + \theta_{y,x} \tag{1}$$

$$\gamma_{xz} = \theta_x - w_{,x}$$

$$\gamma_{yz} = \theta_y - w_{,y}. \tag{2}$$

Figure 1(b) shows the isoparametric system used. We shall also define natural co-ordinate rotations θ_ξ and θ_η in the sense that they define natural co-ordinate based covariant components of what we

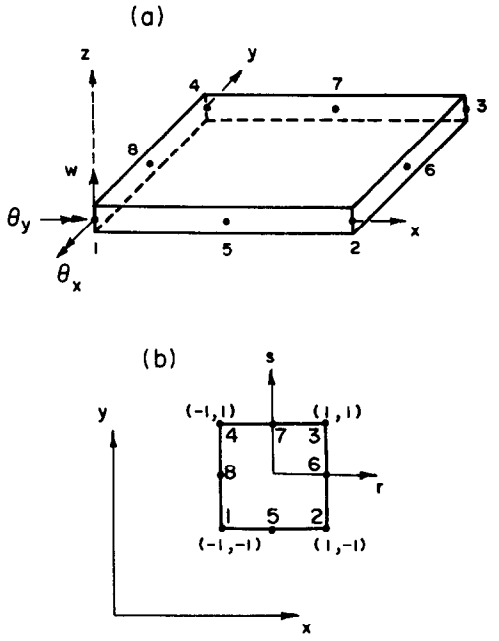

Fig. 1. (a) Geometry of eight-node plate element. (b) Global and natural isoparametric co-ordinate system.

call 'pseudo-shear strains' $\gamma_{\xi\zeta}$ and $\gamma_{\eta\zeta}$ as follows:

$$\gamma_{\xi\zeta} = \theta_\xi - w_{,\xi}$$

$$\gamma_{\eta\zeta} = \theta_\eta - w_{,\eta}. \tag{3}$$

QUAD8-0—the original element

The shape functions for the original serendipity quadratic element are given below. For further reference, we shall describe them as Level 0 functions, with the superscript ^{0} denoting this.

The corner node functions are:

$$N_1^0 = 0.25\{(1-\xi)\eta(\eta-1) - (1-\xi^2)(1-\eta)\}$$

$$N_2^0 = 0.25\{(1+\xi)\eta(\eta-1) - (1-\xi^2)(1-\eta)\}$$

$$N_3^0 = 0.25\{(1+\xi)\eta(\eta+1) - (1-\xi^2)(1+\eta)\}$$

$$N_4^0 = 0.25\{(1-\xi)\eta(\eta+1) - (1-\xi^2)(1+\eta)\}$$

and the mid-side node functions are:

$$N_5^0 = 0.50\{\qquad\qquad (1-\xi^2)(1-\eta)\}$$

$$N_6^0 = 0.50\{(1+\xi)(1-\eta^2)\qquad\qquad\}$$

$$N_7^0 = 0.50\{\qquad\qquad (1-\xi^2)(1+\eta)\}$$

$$N_8^0 = 0.50\{(1-\xi)(1-\eta^2)\qquad\qquad\}. \tag{4}$$

In a conventional displacement model (henceforth QUAD8-0, following the terminology adopted in Ref. [12]) these functions and their derivatives are used directly to interpolate the three field variables w to θ_η in deriving the strains above. An exact integration of all the shear energy terms will now lead to an element that locks severely [5, 6, 12].

Let us now examine how the consistency requirements are met or violated for the covariant shear strain component $\gamma_{\xi\zeta}$ for the QUAD8-0 element. We have

$$\begin{aligned}\theta_\xi = {} & \eta(\eta-1)/2\cdot(\theta_1+\theta_2)/2 + \eta(\eta+1)/2 \\ & \times(\theta_3+\theta_4)/2 + (1-\eta^2)\cdot(\theta_6+\theta_8)/2 \\ & + \eta(\eta-1)/2\cdot\xi\cdot(\theta_2-\theta_1)/2 + \eta(\eta+1)/2 \\ & \times\xi\cdot(\theta_3-\theta_4)/2 + \xi\cdot(1-\eta^2)\cdot(\theta_6-\theta_8)/2 \\ & - (1-\eta)/2\cdot(1-\xi^2)/2\cdot(\theta_1+\theta_2-2\theta_5) \\ & - (1+\eta)/2\cdot(1-\xi^2)/2\cdot(\theta_3+\theta_4-2\theta_7)\end{aligned}$$

$$\begin{aligned}w_{,\xi} = {} & \eta(\eta-1)/2\cdot(w_2-w_1)/2 + \eta(\eta+1)/2 \\ & \times(w_3-w_4)/2 + (1-\eta^2)\cdot(w_6-w_8)/2 \\ & - (\eta-1)/2\cdot\xi\cdot(w_1+w_2-2w_5) + (\eta+1)/2 \\ & \times\xi\cdot(w_3+w_4-2w_7).\end{aligned} \tag{5}$$

In the thin plate limit, the discretized constraints corresponding to the Kirchhoff limit can be associated with principal basis functions as shown in Table 1. It is easy to recognise from Table 1 that the last three constraints are the spurious constraints that can lead to locking (i.e. spurious stiffness that increases indefinitely with increase in value of the penalty multiplier) or to very slow convergence. Our recent studies in [12] showed that this element locked severely and that locking was accompanied by severe spurious linear and quadratic oscillations in the shear stress resultants. We can interpret this in the light of our recent investigations into the linear and quadratic beam elements [17, 18] which showed that inconsistencies in the linear term in the shear strain definition (for the linear beam element) led to 'locking' (i.e. spurious over-stiffening that increases indefinitely with reduction in beam/plate thickness) and spurious linear oscillations in the shear stresses, and inconsistencies in the quadratic term (for the quadratic beam element) led to spurious quadratic shear stress oscillations and to slow convergence but not to 'locking'. Thus the constraints shown in eqns (6g) and (6h) (Table 1) explain the existence of quadratic (i.e. in ξ^2) shear stress oscillations that we have observed in the 'quadratic' QUAD8-0 element and the constraint appearing in eqn (6) accounts for the shear locking and for the linear (i.e. in ξ) shear stress oscillations seen in [12]. Our field-consistency argument therefore identifies this inconsistency in the linear term in ξ

Table 1

Function	Constraint	Nature	Eqn No.
$\eta(\eta-1)/2$	$(w_2-w_1)/2=(\theta_1+\theta_2)/2$	True	(6a)
$(1-\eta^2)$	$(w_6-w_8)/2=(\theta_6+\theta_8)/2$	True	(6b)
$\eta(\eta+1)/2$	$(w_3-w_4)/2=(\theta_3+\theta_4)/2$	True	(6c)
$\xi(1-\eta)/2$	$(w_1-2w_5+w_2)=-\eta(\theta_2-\theta_1)/2$	True	(6d)
$\xi(1+\eta)/2$	$(w_3-2w_7+w_4)=\eta(\theta_3-\theta_4)/2$	True	(6e)
$\xi(1-\eta^2)$	$0=(\theta_6-\theta_8)/2$	Spurious	(6f)
$(1-\eta)/2\cdot(1-\xi^2)$	$0=(\theta_1-2\theta_5+\theta_2)$	Spurious	(6g)
$(1+\eta)/2\cdot(1-\xi^2)$	$0=(\theta_3+2\theta_7+\theta_4)$	Spurious	(6h)

introduced when serendipity shape functions are used to account for the locking here.

Also of significant interest is the fact that the nine-noded rectangular element based on the bi-quadratic Lagrangian functions leads to spurious constraints which are similar to those seen in eqns (6g) and (6h). Numerical experiments show that it does not lock in its exactly integrated form (i.e. its QUAD9-0 form) but has quadratic spurious shear stress oscillations, confirming the use of the analogy from the quadratic beam that inconsistencies at the quadratic term do not lead to locking although they appear as spurious quadratic shear stress oscillations. This leads us to the important clue that the difficulties experienced with the QUAD8 element originate from the special nature of its serendipity interpolations due to the absence of the mid-node, and hence to constraints such as seen in eqn (6f) where a spurious linear inconsistency is seen.

QUAD8-1 to QUAD8-3—elements based on a simple introduction of consistency requirements

In [12], we approached the problem of finding an efficient QUAD8 from a simple understanding of the requirements of field-consistency. We considered the use of field-redistributed substitute shape functions, in a straightforward identification of consistency of terms associated with the polynomial forms, as in [19]. Thus, the original polynomial expansion for a rotation such as θ_ξ will have terms like

$$1 \quad \xi \quad \eta \quad \xi^2 \quad \xi\eta \quad \eta^2 \quad \xi^2\eta \quad \xi\eta^2$$

while the interpolation for $w_{,\xi}$ will have terms like

$$1 \quad \xi \quad \eta \quad \xi\eta \quad \eta^2.$$

One can argue from this that the interpolations for the rotations θ_ξ and θ_η must be smoothed down to the corresponding forms for $w_{,\xi}$ and $w_{,\eta}$ respectively. The variationally correct way to determine the functions which meet this specific field-consistency requirement for isotropic Mindlin plate theory is to smooth the original shape functions in a least squares accurate fashion to the desired form, i.e. to functions that are consistent with the derivative functions [13]. This means that the smoothed functions we must derive for θ_ξ are obtained by smoothing the original functions N^0 to be a least squares form consistent with the shape functions $N^0{}_{,\xi}$: and similarly for θ_η. This operation was simple and resulted in substitute interpolation formulae denoted as the Level 1 functions in [12]. The element based on these functions was designated QUAD8-1.

However, this element locked for certain sets of boundary conditions, even though consistent definitions for the shear stress fields appeared to have been assured within the element domain. Linear oscillations in the shear stress resultants persisted but the quadratic oscillations vanished. The inconsistency in the linear ξ term in the shear strain definitions remained and was the cause of the poor behaviour of this element.

Lower levels of consistency were examined next. First, smoothed shape functions based on the bi-linear form (i.e. having 1, ξ, η and $\xi\eta$ terms only) for the natural co-ordinate rotations were studied in the QUAD8-2 version. This needed the derivative functions defining $w_{,\xi}$ and $w_{,\eta}$ to be smoothed to bi-linear form. Numerical experiments showed that this element was identical in behaviour to the assumed stress mixed element based on the bi-linear shear stress fields [6], and also to the QUAD8 based on a $2*2$ Gaussian integration of the shear strain energy. It locked, showing the same linear shear stress oscillations seen in QUAD8-1 above. Thus smoothing to Level 2 had failed to remove the same inconsistency associated with the linear ξ term of the assumed shear strain definitions that we had noticed in Level 1 earlier.

At the next lower level, a linear form (i.e. having 1, ξ and η only) was chosen for the natural co-ordinate rotations and, correspondingly, the derivative functions defining $w_{,\xi}$ and $w_{,\eta}$ were also smoothed to linear form. Numerical experiments below show that this element is similar in behaviour to the assumed stress mixed element based on the linear shear stress fields [6]. It did not lock in quadrilateral form for all the boundary conditions considered, i.e. its accuracy is insensitive to a very large variation in the thickness of the plate and to distortion of the element. The element also produces accurate transverse shear stress resultants at the centroid. Spectral analysis revealed that this element has two spurious zero-energy modes in addition to the usual three rigid body modes. In certain, rarely encountered, situations, the zero-energy mechanisms introduced can

'act-up', but in most practical situations, this is not a very debilitating influence.

QUAD8-4—the element based on line-consistency of shear strains associated with principal basis functions

We saw above that deriving the assumed strain fields in an orthogonal or variationally correct fashion resulted in an efficient element only at a level which also introduced two zero-energy modes. Donea and Lamain have cleverly shown that one way to identify a workable set of consistency requirements is to isolate the principal forms of the basis functions which appear when the derivatives such as $w_{,\xi}$ and $w_{,\eta}$ are derived. They, however, seek to establish consistency for the Cartesian shear strain components and hence obtain smoothed functions for $x_{,\xi}\,\theta_x$ and $y_{,\xi}\,\theta_y$ terms for γ_{xz}, etc. It should therefore be possible for us to derive an element that achieves consistency in the functions for the covariant components of the shear strains in the same manner.

We must look for a substitute assumed function for the rotation θ_ξ in the following form:

$$\theta_\xi = \eta(\eta-1)/2\cdot A_1 + \eta(\eta+1)/2\cdot A_2 + (1-\eta^2) \times A_3 + \xi(1-\eta)/2\cdot A_4 + \xi(1+\eta)/2\cdot A_5. \quad (7)$$

We must determine the constants A_1 to A_5 in a logical manner. Hinton and Huang [8] perform this sampling at a set of five points, the two Gauss points ($\xi = \pm 1/\sqrt{3}$) on the reference lines $\eta = \pm 1$ and the mid-point ($\xi = 0$) on the line $\eta = 0$. Donea and Lamain [9] need to determine very similar smoothed polynomial functions for the $x_{,\xi}\,\theta_x$ and $y_{,\xi}\,\theta_y$ functions and adopt the alternative strategy of determining these as mean value approximations of the original functions on the principal reference lines.

On adopting this latter strategy, the appropriate smoothed function for θ_ξ in $\gamma_{\xi\zeta}$ is:

$$\theta_\xi = \eta(\eta-1)/2\cdot(\theta_1+4\theta_5+\theta_2)/6 + \eta(\eta+1)/2 \times(\theta_3+4\theta_7+\theta_4)/6 + (1-\eta^2) \times[(\theta_6+\theta_8)/2 - (\theta_1-2\theta_5+\theta_2+\theta_3-2\theta_7+\theta_4)/6] + \eta(\eta-1)/2\cdot\xi\cdot(\theta_2-\theta_1)/2 + \eta(\eta+1)/2\cdot\zeta\cdot(\theta_3-\theta_4)/2$$

so that the constraints can be related as in Table 2. Equations (8a)–(8e) (Table 2) are all true constraints now, and this accounts for the complete freedom from locking.

Transformation from covariant base to Cartesian base

The definitions of components of the shear strain tensor have been made in the covariant base.

Table 2

Function	Constraint	Eqn No.
$\eta(\eta-1)/2$	$(w_2-w_1)/2 = (\theta_1+4\theta_5+\theta_2)/6$	(8a)
$(1-\eta^2)$	$(w_6-w_8)/2 = (\theta_6+\theta_8)/2 - (\theta_1-2\theta_5+\theta_2+\theta_3 - 2\theta_7+\theta_4)/6$	(8b)
$\eta(\eta+1)/2$	$(w_3-w_4)/2 = (\theta_3+4\theta_7+\theta_4)/6$	(8c)
$\xi(1-\eta)/2$	$(w_1-2w_5+w_2) = (\theta_2-\theta_1)/2$	(8d)
$\xi(1+\eta)/2$	$(w_3-2w_7+w_4) = (\theta_3-\theta_4)/2$	(8e)

The transformation from the natural co-ordinate definitions to the Cartesian co-ordinate definitions must preserve the constraints consistently, even in an arbitrarily distorted quadrilateral. References [12] and [16] have identified that the simplest way to perform this is to interpolate only the natural co-ordinate based shear strains within the element using the smoothed shape functions derived earlier, but make the necessary co-ordinate transformations only at the element nodes. This secures, more realistically, the consistency of definitions of shear strains on an edge from the two elements forming it.

QUAD8-5—element based on mixed interpolations

In Hinton and Huang [8], the assumed shear strains are extrapolated from a set of unique points, i.e. $\gamma_{\xi\zeta}$ and $\gamma_{\eta\zeta}$ need a set of five points each to define functions complete in the Level 1 sense. Interestingly, this element does not lock, like QUAD8-4, and has no zero-energy modes. However, this element provides more flexible answers than QUAD8-3 and QUAD8-4 for most applications, converging more slowly from above than the QUAD8-3 or QUAD8-4 does for most applications. We can attribute this to the fact that these mixed interpolations for the assumed shear strain functions are not orthogonal to the difference in the shear strains derived directly from the displacements and rotations and the shear strain operators and the assumed shear strains. Thus the exact equivalence of the assumed shear strain method to the Hellinger–Reissner variational basis is lost [13], and leads to this poorer performance as compared to the QUAD8-3, where the constants for the assumed shear strain functions are derived using the *a priori* administration of the orthogonality condition as the basis [13]. Its poorer performance relative to the QUAD8-4 element must be explained from the fact that line consistency in the QUAD8-4 element is established by an equivalent least squares or mean value averaging of tangential shear strains along appropriate reference lines, whereas in QUAD8-5, this is done using sampling at five specified points. While these are exactly equivalent on lines $\eta = \pm 1$ and $\xi = \pm 1$ for the respective transverse shear strains, they are not so on lines $\eta = 0$ and $\xi = 0$. It is instructive to examine this distinction here. The adoption of Hinton and Huang's procedure to sampling at five points will lead to the following change in the coefficient associated with the basis

function $(1-\eta^2)$ (i.e. corresponding to the reference line $\eta = 0$) as

$$\theta_\xi = \eta(\eta-1)/2 \cdot (\theta_1 + 4\theta_5 + \theta_2)/6 + \eta(\eta+1)/2 \times (\theta_3 + 4\theta_7 + \theta_4)/6 + (1-\eta^2) \times [(\theta_6+\theta_8)/2 - (\theta_1 - 2\theta_5 + \theta_2 + \theta_3 - 2\theta_7 + \theta_4)/4] + \eta(\eta-1)/2 \cdot \xi \cdot (\theta_2 - \theta_1)/2 + \eta(\eta+1)/2 \cdot \xi \cdot (\theta_3 - \theta_4)/2.$$

Comparing this with eqn (8b), we notice that the value 6.0 has now been replaced by a value 4.0. This difference leads to a noticeable loss of accuracy in the QUAD8 element of Hinton and Huang.

QUAD8-6—the Donea and Lamain element

The logic of the covariant based QUAD8-4 element introduced above departs slightly from that for Donea and Lamain's element [9], and in rectangular form, both elements will be identical.

In the covariant based approach [12] the interpolations for the Cartesian system based shear strains are made in terms of the nodal displacements and Cartesian co-ordinate based rotations, the Jacobean terms, also at the nodes and the interpolations from the nodal values using the specially determined smoothed interpolation forms (N_ξ) and (N_η). We postulated that this strategy will preserve the consistency of the shear strain definitions even in a Cartesian base for a general distortion of the quadrilateral.

Donea and Lamain's logic is now to write the Cartesian based shear strains as

$$\gamma_{xz} = y_{,\eta}/|J|\, P_\xi - y_{,\xi}/|J|\, P_\eta$$

$$\gamma_{yz} = -x_{,\eta}/|J|\, P_\xi + x_{,\xi}/|J|\, P_\eta \qquad (9)$$

$$P_\xi = (x_{,\xi}\theta_x + y_{,\xi}\theta_y - w_{,\xi})$$

$$P_\eta = (x_{,\eta}\theta_x + y_{,\eta}\theta_y - w_{,\eta}). \qquad (10)$$

Donea and Laman now state that 'the problem of obtaining free of locking behaviour in C° plate elements amounts to properly designing the above two polynomials.

In order to denote clearly how consistency is to be obtained, we make a distinction between what we shall call the inconsistent definitions of P_ξ^0 and P_η^0 which are obtained by directly substituting the interpolations for $x_{,\xi}\theta_x$, $y_{,\xi}\theta_y$, $x_{,\eta}\theta_x$ and $y_{,\eta}\theta_y$ and the consistent forms P_ξ^1 and P_η^1 which are now suitably smoothed so that they are consistent with $w_{,\xi}$ and $w_{,\eta}$ forms respectively. These are obtained as mean value approximations of the original forms P_ξ^0 and P_η^0 on the principal reference lines.

Generation of stiffness matrices

All versions of this element are obtained by using a uniform numerical integration based on the $3*3$ Gaussian rule for all energy terms. The unconstrained energy terms, in this case the bending energy terms, are derived from the original shape function definitions, as also are the consistent load vectors and the mass matrices. Only in the computation of the shear stiffness matrix, is the need for the use of the field-reconstituted shear strain definitions observed.

ACCURATE SHEAR RECOVERY FROM THE NON-ORTHOGONAL LINE-CONSISTENT ELEMENTS

A recent study of non-orthogonal assumed strain procedures for the quadratic and cubic shear deformable beam elements [15] and for the eight-node line-consistent plate elements [20] showed that these elements gave reasonably accurate displacement solutions but poor stress predictions. These are due to spurious stress oscillations which can be related to the presence of artificially created spurious load mechanisms. Such mechanisms can be traced to the non-orthogonality of these assumed strain fields and to the subsequent loss of an exact variational equivalence to the corresponding Hellinger–Reissner or Hu–Washizu principles.

It was found in [20] that spurious linear and quadratic shear stress oscillations were induced due to the non-orthogonal nature of the shear strain definitions in the various line-consistent elements (i.e. QUAD8-4, QUAD8-5 and QUAD8-6 here). It was also demonstrated therein that by a suitable filtering procedure involving a least squares smoothing of the shear strain fields into a bi-linear form and then sampling this smoothed form only at the centroids, it was possible to obtain transverse shear stress resultants at element centroids which were of accuracy commensurate with the high performance these elements had in displacement predictions. This filtering procedure will be used to report the transverse shear stress resultants in this paper for the various numerical examples studied.

NUMERICAL EXPERIMENTS

We shall direct our numerical studies to bring out the similarities and differences between the four versions of the eight-noded element that we have discussed so far. While QUAD8-3 is based on field-consistency requirements alone but is a variationally correct or orthogonal formulation, the other three take into account, principally, the consistency of the tangential shear strain definitions on the edge lines and are therefore not variationally correct. That is, these are the so-called non-orthogonal formulations. The benchmark tests to be used are therefore those that can demonstrate how these elements behave in general meshes. It is important to demonstrate here the accuracy with which the line-consistent

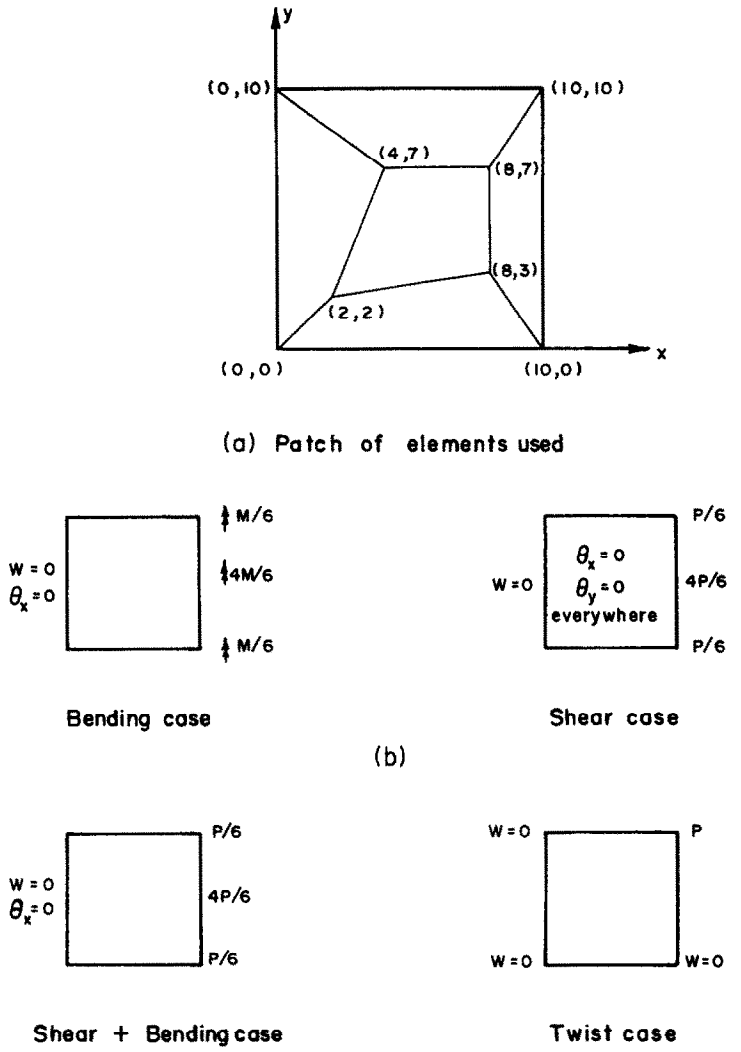

Fig. 2. Constant strain patch tests.

elements pass through the constant strain patch tests, in contrast to the results of [20] which show that these elements give poor shear stress resultants in conjunction with very accurate displacement fields for standard test examples such as the uniformly loaded cantilever beam or the simply supported plate. This was traced to the non-orthogonal nature of such formulations. The optimal way of recovering more accurate shear stress resultants [20] is now used to determine all shear stress resultants.

Constant strain patch tests

The most frequently used patch test is a configuration of five arbitrary quadrilateral elements as shown in Fig. 2. The dimensions of the plate are $L = 10$ and $b = 10$, and thicknesses $t = 1.0$ and 0.001 are considered. The elastic properties are $E = 10^6$ and $\mu = 0.0$, the latter value allowing comparisons to be made directly with elementary beam theory solutions.

We shall consider four types of straining configurations as discussed in the sub-sections below.

Constant bending strain test. A distributed edge couple of constant intensity on the free edge is simulated by three concentrated edge couples of intensity $M/6$, $4M/6$ and $M/6$ at the three nodes on the free edge as shown in Fig. 2(b). At the fixed edge, w and θ_x are suppressed to give the clamped edge conditions.

The non-dimensional deflection $wEbt^3/ML^2$ at the free edge according to thin beam theory should be 6.00. It can be seen from Table 3 that QUAD8-3 can pass this test only in a qualified sense whereas all the other three elements do so exactly. These three elements can also produce exactly correct constant bending stress resultants $M_x = M$ over all five elements in the patch. We can attribute this to the satisfaction of line-consistency of the tangential shear strains on element edge lines for QUAD8-4, QUAD8-5 and QUAD8-6.

Constant shear strain test. A uniformly distributed edge load is simulated by three concentrated loads as shown in Fig. 2(b). Note that the imposed conditions

imply that all rotations are zero and that only pure shear is possible. No field-inconsistency problem can therefore manifest itself here and, as expected, all four versions pass this simple test.

If a shear factor $k = 1.0$ is used to estimate the shear strain energy, the theoretical non-dimensional tip deflection is $wEbt/PL = 2.0$. We see from Table 4 that all four element versions succeed in producing this value accurately. Again, the shear stress resultant Q_{xz} is correctly recovered in all these cases.

It is in this form that this test is used in the literature and it is clear from the present experiment that this test fails to bring out the essential nature of the inconsistency problems faced by the various versions of the element. In the next sub-section, we offer a more useful patch test to highlight this feature.

Constant shear and linear bending strain test. To understand more realistically how field-inconsistencies are induced under shearing, the shear test is repeated allowing the rotations θ_x to develop. This corresponds to a constant shear and linear bending strain patch test.

From Table 5, we see that both QUAD8-4 and QUAD8-6 give estimates which are very close to the theoretical values. However, both QUAD8-3 and QUAD8-5 are much less accurate. We can attribute the deficiency in QUAD8-3 to the lack of edge-consistency and the deficiency in QUAD8-5 to the approximation made when the tangential shear strains on the $\eta = 0$ and $\xi = 0$ lines are sampled at the single point instead of being represented in a mean-value or least squares sense on these lines.

Constant twisting strain test. The plate is now supported at three corner points and is loaded by a concentrated shear force at the fourth corner. Classical thin plate theory predicts that a pure constant state of twisting strain is developed in the patch. For a thin plate (thickness $t = 0.001$ in.) for which an exact prediction is available, it is seen that QUAD8-4, QUAD8-5 and QUAD8-6 all pass with flying colours and only QUAD8-3 shows relatively poorer performance (Table 6).

Single element cantilever beam

With reference to Fig. 1, consider a single element cantilever beam clamped at nodes 1, 8 and 4. The beam is of length $L = 10$, width $b = 10$ and thickness $t = 0.1$. Young's modulus is taken as $E = 10^6$ and $\mu = 0.0$. Reference [20] has shown that the critical loading case which activates spurious loading mechanisms due to non-orthogonality of assumed shear strain definitions is that of a uniformly distributed load of intensity q. Table 7 shows the non-dimensional tip deflection parameters at nodes 2, 6 and 3 for this load case for the four elements QUAD8-3 to QUAD8-6. QUAD8-3, which is orthogonally correct, produces the exact tip deflections and reproduces exactly the linear variation in shear stress resultant Q_{xz} along the length of the beam, and gives an accurate least squares correct linear fit of the actual quadratic variation in bending moment resultant M along x (not shown). These values are therefore exact on the Barlow lines $\xi = \pm 1/\sqrt{3}$ in this case.

The deflections at the free edge for the QUAD8-4, QUAD8-6 and QUAD8-5 models show errors according to set patterns. QUAD8-4 and QUAD8-6, as expected, give identical results in this rectangular form. The tip deflections on the free edge reveal an exactly parabolic departure from the correct value (i.e. here taken as 1.50012 to account for shear deformability), showing that at the Gauss points $\eta = \pm 1/\sqrt{3}$ on this edge, they are correct. Drawing our analogy from the studies of the non-orthogonally formed beam elements, we can attribute this to the spurious stress oscillations resulting from the spurious load mechanisms activated by the uniformly distributed load for these non-orthogonal formulations.

QUAD8-5 deflections on the free edge also show a parabolic variation, but about an incorrect value of the tip deflection. This suggests that the errors due to excessive flexibility caused by the loss of accuracy involved in five-point sampling are compounded by the stress oscillations caused by the spurious load mechanisms arising from the non-orthogonal nature of the assumed shear stress strain fields.

Figure 3 shows the stress predictions made by the QUAD8-4 and QUAD8-6 models. The linear variation of M along x that is permitted by a quadratic element is captured directly, and is the same as for the QUAD8-3 model. However, there is now an additional spurious quadratic oscillation in the y direction due to the spurious load mechanisms. Thus, in this case, we have the fortuituous result that at the Barlow points ($\xi = \pm 1/\sqrt{3}$, $\eta = \pm 1/\sqrt{3}$) the values of the moment resultant M are as per theory.

The effect of the spurious load mechanisms is now more noticeably felt in the predictions of the transverse shear stress resultant Q_{xz}. There are severe quadratic oscillations about the correct theoretical value, and on lines $\eta = \pm 1/\sqrt{3}$, these elements give the correct answers (Fig. 3). When the filtering technique is used (i.e. using a least squares smoothed bi-linear fit of the shear stresses) the correct values are obtained.

Bending of simply-supported square plate—uniform mesh

Displacement predictions. We study the square plate with what are called the 'hard' simple support (SS2) conditions (the tangential rotations on a supported edge are also suppressed) under uniformly distributed load of intensity q. Symmetry allows a quarter of the plate to be modelled. We report in Table 8 the displacement w at the centre of the plate of rigidity D, side length a and thickness h from a $2 * 2$ grid of all four versions of QUAD8. It is seen that none of the elements lock. Versions QUAD8-3, QUAD8-4 and QUAD8-6 show identical levels of

Table 3. Tip deflections ($wEbt^3/ML^2$) for constant bending strain patch test

t	Node	QUAD8-3	QUAD8-4	QUAD8-5	QUAD8-6	Theory
1.0	18	5.53	6.00	6.00	6.00	
	19	5.46	6.00	6.00	6.00	
	20	5.43	6.00	6.00	6.00	
						6.00
0.001	18	5.34	6.00	6.00	6.00	
	19	5.23	6.00	6.00	6.00	
	20	5.22	6.00	6.00	6.00	

Table 4. Tip deflections ($wEbt/PL$) for constant strain patch test

t	Node	QUAD8-3	QUAD8-4	QUAD8-5	QUAD8-6	Theory
1.0	18	2.00	2.00	2.00	2.00	
	19	2.00	2.00	2.00	2.00	
	20	2.00	2.00	2.00	2.00	
						2.00
0.001	18	2.00	2.00	2.00	2.00	
	19	2.00	2.00	2.00	2.00	
	20	2.00	2.00	2.00	2.00	

Table 5. Tip deflections ($wEbt^3/PL^3$) for constant shear and linear bending strain patch test

t	Node	QUAD8-3	QUAD8-4	QUAD8-5	QUAD8-6	Theory
1.0	18	3.80	4.08	4.00	4.02	
	19	3.76	4.11	4.05	4.02	
	20	3.74	4.08	3.98	4.01	
						4.00
0.001	18	3.66	3.99	3.65	3.99	
	19	3.59	4.04	3.77	4.00	
	20	3.57	3.99	3.68	3.99	

Table 6. Tip deflections (wEt^3/PL^2) for constant twist patch test

t	Node	QUAD8-3	QUAD8-4	QUAD8-5	QUAD8-6	Theory
1.0	18	0.00	0.00	0.00	0.00	
	19	3.29	3.22	3.21	3.22	
	20	6.58	6.42	6.41	6.45	
0.001	18	0.00	0.00	0.00	0.00	0.00
	19	2.98	3.00	3.00	3.00	3.00
	20	5.99	6.00	6.00	6.00	6.00

Table 7. Non-dimensional tip deflection parameters for single element cantilever beam

Parameter	Node	QUAD8-3	QUAD8-4	QUAD8-5	QUAD8-6	Theory
wEt^3/qL^4	2	1.50012	1.46688	1.72108	1.46688	
	6	1.50012	1.51674	1.86107	1.51674	1.5
	3	1.50012	1.46688	1.72108	1.46688	

accuracy. However QUAD8-5 shows relatively poorer accuracy which can again be attributed to the approximations resulting from the use of the single sampling point to derive the tangential shear strains on the lines $\eta = 0$ and $\xi = 0$.

Stress predictions. A closely examined study of the stress resultants in [10] has shown that the shear stress resultants obtained by directly using the assumed shear strain interpolations for the stress recovery depart considerably from the theoretical values. It is seen that there are large quadratic oscillations which are superimposed on large linear oscillations. The filtering strategy recommended in [20] smooths the original shear strain interpolations into a smoothed

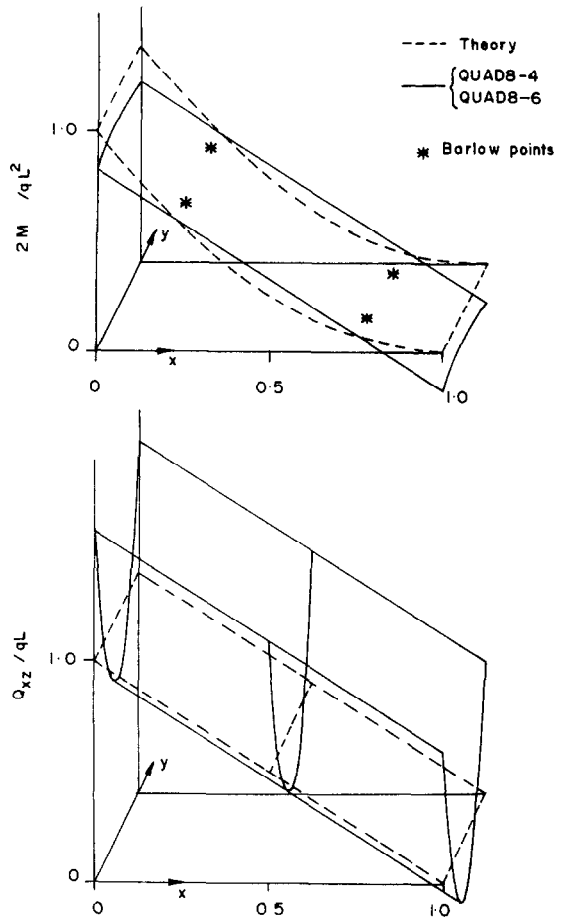

Fig. 3. Stresses in QUAD8-4 and QUAD8-6 single element cantilever under u.d.l.

bi-linear fit and the value sampled at the centroids of the elements using this smoothed fit gives the true shear stress resultants.

Figure 4 shows the application of this filtering strategy to a $4 * 4$ uniform mesh of the same problem. Figure 4(a) shows the shear stress resultant σ_{xz} on $y/a = 0$ from a QUAD8-3 mesh. The shear stress resultants are extrapolated from the centroids of the elements to the line $y = 0$ and these are compared with the prediction made by thin plate theory. The agreement is very good, showing that the orthogonally derived field consistent element has no difficulties in providing accurate stresses. Figure 4(b) shows the stress resultants taken from the nodes of a QUAD8-4 mesh before filtering. Spurious linear and quadratic shear stress oscillations induced by the non-orthogonality of the formulations are now present. Figure 4(c) shows that the extrapolation of values from the centroids of these elements before filtering to the edges of the elements on the line $y = 0$ shows that linear oscillations remain in such a procedure. Therefore, to eliminate this, the correct filtering technique involves making a smoothed bi-linear fit of the shear stresses and extrapolating the centroidal values from this filtered field to lines of interest. Figure 4(d) shows that the accuracy obtained by this filtering technique now matches that obtained with the variationally correct QUAD8-3.

Square simply-supported (SS2) plate—distorted meshes

It is well known that the earlier forms of the QUAD8 element were very sensitive to distortion in terms of shape (deviation from rectangle) or shift in mid-side nodes away from the actual location of the mid-side. We shall now examine the behaviour of the four versions considered here under such distortions. Figure 5 shows the various grids used. Mesh A shows the regular uniformly spaced $2 * 2$ grid of the quarter part of a plate of sides $a = 10$ in. In Mesh B, the nodes marked by crosses are shifted as follows—(9, 13) by 2Δ in., (6, 8, 10, 12, 14, 16) by Δ in., so that the element shapes are distorted but the mid-nodes remain at the mid-side. Meshes C and D are variations of these. In C, an irregular mesh is obtained with nodes (6, 8, 14, 16) now as in A, leading to a shift of the nodes from the exact mid-side. In D, the grid is regular but the nodes (6, 8, 14, 16) are shifted as in B. In Mesh E, we shall experiment with a case where the edges allow a parabolic curvature.

Table 7 gives the results obtained when the plate thickness is reduced. Meshes B, C and D use distortions corresponding to $\Delta = 0.25$ and Mesh E uses $\Delta = 0.5$ in. Both mid-side node shift and distortion from rectangular shape do not lead to large errors at very low thickness ratios in all the four versions of QUAD8 considered here, i.e. no sensitivity to locking even at very small thickness ratios. The sequence of definitions of shear strains and transformations followed in these cases have correctly retained the required consistency of the shear strain definitions.

CONCLUSIONS

In this paper we have examined the conflict introduced by the field- and line-consistency requirements for an eight-node plate bending element based on the

Table 8. Central deflection $(wD/qa^4) * 10^2$ for $2 * 2$ grid of isotropic square simply supported (SS2) plate

t	QUAD8-3	QUAD8-4	QUAD8-5	QUAD8-6	Theory
0.1000	0.4238	0.4231	0.4384	0.4231	0.427
0.0100	0.4062	0.4062	0.4196	0.4062	0.406
0.0010	0.4060	0.4060	0.4194	0.4060	0.406
0.0001	0.4060	0.4060	0.4194	0.4060	0.406

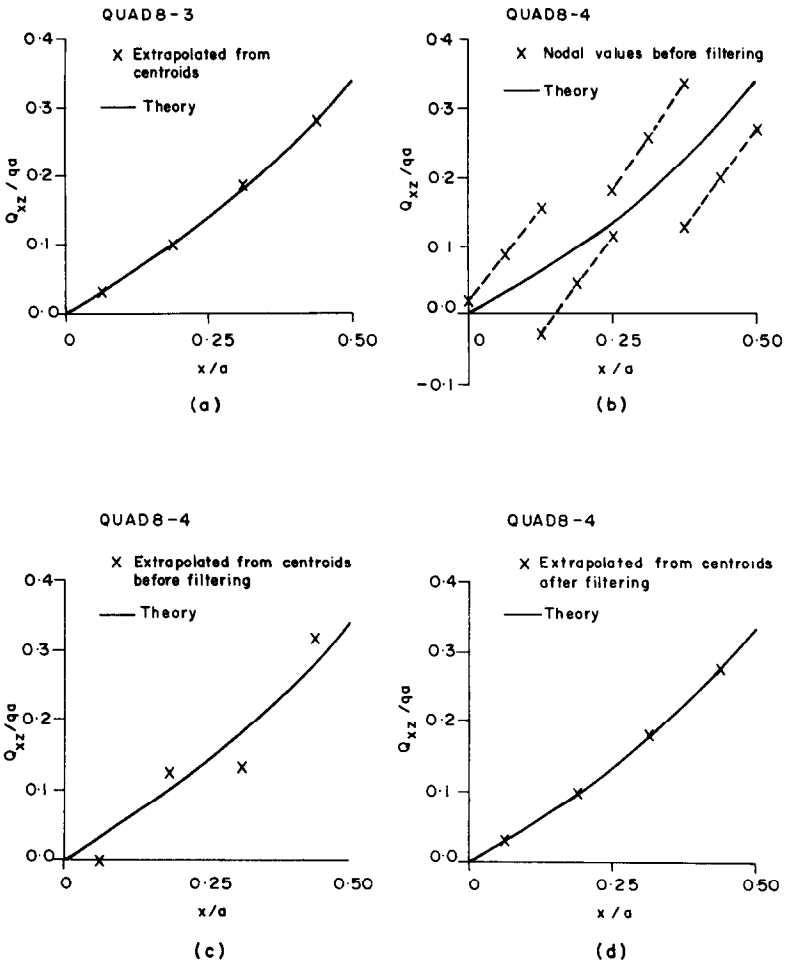

Fig. 4. Q_{xz} on $y = 0$ of a 4×4 mesh of a quarter of an SS plate under u.d.l.

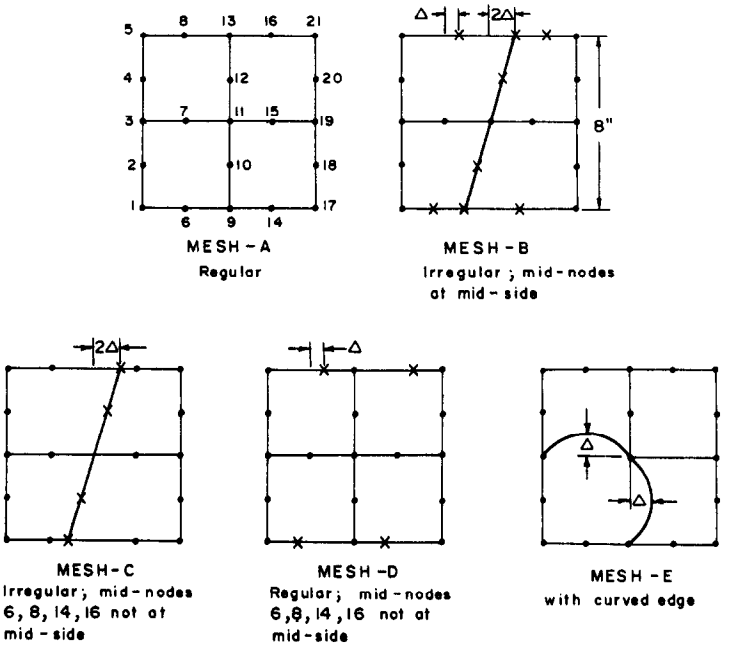

Fig. 5. Regular and irregular meshes for 2×2 grid of a square SS2 plate.

Table 9. Central deflection $(wD/qa^4) * 10^2$ for regular and distorted 2 * 2 QUAD8-3 meshes of isotropic simply supported plate (Fig. 3)

Mesh	h/a	QUAD8-3	QUAD8-4	QUAD8-5	QUAD8-6
B	0.1000	0.4293	0.4278	0.4449	0.4264
	0.0100	0.4077	0.4071	0.4202	0.4059
	0.0010	0.4074	0.4068	0.4199	0.4057
	0.0001	0.4074	0.4068	0.4199	0.4057
C	0.1000	0.4332	0.4265	0.4499	0.4225
	0.0100	0.4045	0.4045	0.4186	0.4016
	0.0010	0.4036	0.4042	0.4186	0.4016
	0.0001	0.4036	0.4042	0.4178	0.4014
D	0.1000	0.4210	0.4263	0.4350	0.4299
	0.0100	0.3917	0.4052	0.4128	0.4096
	0.0010	0.3906	0.4050	0.4125	0.4094
	0.0001	0.3906	0.4050	0.4125	0.4094
B	0.1000	0.3965	0.4267	0.4388	0.4186
	0.0100	0.3664	0.4035	0.4150	0.3986
	0.0010	0.3656	0.4033	0.4148	0.3984
	0.0001	0.3656	0.4033	0.4147	0.3984

serendipity functions. Thus, a line-consistency formulation implied in procedures like that used by Hinton and Huang [8] or Donea and Lamain [9] or for the QUAD8-4 element here violates the orthogonality condition required for the assumed strain interpolations. The stress oscillations introduced due to this can be carefully filtered out and the element thus implemented is a useful one.

Acknowledgements—The authors are extremely thankful to Prof. R. Narasimha, Director, National Aeronautical Laboratory and to Dr B. R. Somashekar, Head of Structures Division, for their constant encouragement and interest in the subject.

REFERENCES

1. R. D. Mindlin, Influence of rotary inertia and shear on flexural motions of isotropic elastic plates. *J. appl. Mech.* **18,** 31–38 (1951).
2. S. Ahmad, B. M. Irons and O. C. Zienkiewicz, Analysis of thick and thin shell structures by curved elements. *Int. J. Numer. Meth. Engng* **2,** 419–451 (1970).
3. O. C. Zienkiewicz, R. L. Taylor and J. M. Too, Reduced integration techniques in general analysis of plates and shells. *Int. J. Numer. Meth. Engng* **3,** 545–586 (1971).
4. S. E. Pawsey and R. W. Clough, Improved numerical integration of thick shell finite elements. *Int. J. Numer. Meth. Engng* **3,** 545–586 (1971).
5. E. D. L. Pugh, E. Hinton and O. C. Zienkiewicz, A study of quadrilateral plate bending elements with reduced integration. *Int. J. Numer. Meth. Engng* **12,** 1059–1079 (1978).
6. S. W. Lee and T. H. H. Pian, Improvement of plate and shell finite elements by mixed formulations. *AIAA Jnl* **16,** 29–34 (1978).
7. K. J. Bathe and E. N. Dvorkin, A formulation of general shell elements—the use of mixed interpolation of tensorial components. *Int. J. Numer. Meth. Engng* **22,** 697–722 (1986).
8. E. Hinton and H. C. Huang, A family of quadrilateral Mindlin plate elements with substitute shear strain fields. *Comput. Struct.* **23,** 409–431 (1986).
9. J. Donea and L. G. Lamain, A modified representation of transverse shear in C^0 quadrilateral plate elements. *Comput. Meth. appl. Mech. Engng* **63,** 183–207 (1987).
10. G. P. Prathap, Field-consistent finite element formulations. Interner Bericht IB 131-84/33, DFVLR, Institut fur Strukturmechanik, Braunschweig, West Germany (1984).
11. G. P. Prathap, Field-consistency and the finite element analysis of multi-field structural problems. In *Analysis of Structures* (Edited by K. A. V. Pandalai and B. R. Somashekar). NAL-SP-RTP-1/84. National Aeronautical Laboratory, Bangalore, India (1984).
12. G. Prathap, B. P. Naganarayana and B. R. Somashekar, Field-consistency analysis of the isoparametric eight-noded plate bending element. *Comput. Struct.* **29,** 857–874 (1988).
13. G. Prathap, The variational basis for least squares field-redistribution of strain functions in the finite element formulation of constrained media elasticity. TM ST 8801, National Aeronautical Laboratory, Bangalore, India (1988).
14. J. C. Simo and T. J. R. Hughes, On the variational foundations of assumed strain methods. *J. appl. Mech.* **53,** 51–54 (1986).
15. G. Prathap and B. P. Naganarayana, Stress oscillations, spurious load mechanisms in non-orthogonal assumed strain formulations. TM ST 8804, National Aeronautical Laboratory, Bangalore, India (1988).
16. G. Prathap and B. R. Somashekar, Field- and edge-consistency synthesis of a four-noded quadrilateral plate bending element. *Int. J. Numer. Meth. Engng* **26,** 1693–1708 (1988).
17. G. Prathap and C. Ramesh Babu, A linear thick curved beam element. *Int. J. Numer. Meth. Engng* **23,** 1313–1328 (1986).
18. G. P. Prathap and C. Ramesh Babu, Field-consistent strain interpolations for the quadratic shear flexible beam element. *Int. J. Numer. Meth. Engng* **23,** 1973–1984 (1986).
19. G. Prathap, A C^0 continuous four-noded cylindrical shell element. *Comput. Struct.* **21,** 995–999 (1985).
20. G. Prathap and B. P. Naganarayana, Consistency and orthogonality requirements and accurate stress recovery from the assumed strain eight-node quadrilateral plate bending elements. TM ST 8805, National Aeronautical Laboratory, Bangalore, India (1988).